CAPACITIVE SENSOR FOR DYNAMIC GAS-LIQUID PHASE DETECTION IN TWO-PHASE FLOWS

Niederauer Mastelari
Marc Zwanziger
Eugênio Spanó Rosa
Faculdade de Engenharia Mecânica da Universidade Estadual de Campinas. Campinas - SP, Brasil. CEP 13083-970.
niede@fem.unicamp.br, marczzztoo@yahoo.com.br, erosa@fem.unicamp.br

Abstract: *The main purpose of the developed capacitive sensor is to access, in actual oil pipelines, the sizes, the velocities and the frequencies of the gas-oil structures occurring in the slug flow pattern. The probe is intrusive. It consists of a single rod of stainless steel crossing a metallic tube along the diameter line. The rod is insulated from the pipe. The sensor works by measuring the capacitance between the rod and the pipe wall. The gas and the oil phases are detected due to the changes on the dielectric constants of the media. This paper describes the characteristics of the sensor, including its sensitivity, its circuit block diagram, and the static and dynamic tests in gas-oil pipelines with sizes of 29mm and 150mm in diameter.*

Key Words*: capacitive sensor, slug flow, two-phase flow, phase detection*

1. Introduction

The arising of new scenarios for oil production in Brazil, with high viscosity crude, or the constant increase of water production on mature oil fields, is a challenge to flow assurance and flow production engineering. These two scenarios have in common the slug flow pattern (the most frequent flow pattern in oil production) and high viscosity liquid phase. The challenging aspect sits on the fact that still today the slug flow properties are poorly understood for high viscous liquids jeopardizing the flow prediction for these new scenarios. To overcome of some of these difficulties an experimental program was launched to better understand how the liquid viscosity affects the gas-oil structures in size, velocity and frequency.

The test campaign resorts with an indoor experimental facility as well as actual gas-oil pipelines. The capacitive sensor was considered the best option to work with dielectric liquid of high viscosity. Actually, capacitive sensors are frequently used in gas-liquid flow, operating in low pressure and mostly with water or another low-viscosity liquid. They efficiently measure the two-phase flow properties (void fraction, film thickness, flow regime detection or just phase detection) of isothermal gas-liquid flows, as well as of phase-change flows, such as evaporating or condensing phenomena (Merilo et al., 1977, Masuda et al., 1980, and Heerens, 1986). These capacitive sensors were mostly developed as non-intrusive devices, rendering the void fraction doing the time average of the signals or the flow pattern if instant signals are employed. A variety of electrode configurations have been designed by a number of researchers, ranging from parallel flat plate to multiple helical wounds (Abouelwafa and Kendall, 1980). In all of them, the electrodes have to be isolated from the fluid and assembled in dielectric pipes. The capacitance variation is due to the dielectric change of the media as the gas or the liquid passes through the volume sensed by the electrodes. The signal linearity with the phase content of the volume depends on the electrode configuration, but in most cases it is linear. The typical capacitance value ranges from 0.1 pF to 10 pF, demanding proper shielding against stray capacitance and a good signal-to-noise ratio. Two recent developments employing concave parallel electrodes are in Duarte and Prata (2002) and in Reis and Goldstein (2003). The former develops the capacitive sensor to void fraction measurements of a refrigerant flow, in a glass pipe of small diameter, and the other use it to measure the shape of elongated bubbles occurring in slug regime of air-water flow, in a Plexiglas pipe.

Despite the advantages of the non-intrusive family of capacitive sensors, they are not suited to in-site applications on gas-oil lines, due to the requirement of a non-metallic pipe to house the probes. The oil production rigs frequently work with pressurized lines, which, for safety reasons, forbidden the use of non-metallic pipes. A new intrusive capacitive probe was developed to withstand the field pressure, temperature and safety requirements. The probe consists of a single rod of stainless steel, crossing the pipe along the diameter line, see Fig. 1. The rod is insulated from the pipe and the sensor works by measuring the capacitance between the rod and the pipe wall. This new configuration surpasses the dielectric pipe restriction, once the pipe itself is part of the capacitor. Clearly one of the disadvantages is its intrusive nature, which may interfere with the flow field. Nonetheless, it is simple to build, easy to install, does not require guard electrodes neither electrostatic shield, because the pipe itself is the shield. This paper starts describing the probe itself. Then, it shows a numerical and analytical analysis of the electrostatic potential field on the rod's neighborhood. The circuit block diagram is presented in sequence and finally, the static and dynamic tests with petroleum and gas, within 29 mm and 150 mm diameter pipes are shown.

2. Probe description

The capacitive probe consists of a stainless steel rod and a metallic pipe. The rod crosses the pipe transversally by a line coincident with the pipe diameter line. The rod is kept in place inside the pipe through two pinch points, which, at the same time, keep it electrically insulated from the pipe (Fig. 1). The definition of the rod diameter is not a simple question. To reduce the hydrodynamic rod's interference one would require the smallest diameter possible, but as the rod's diameter decreases, so decreases its capacitance level, as well as its mechanical strength to withstand the crossing stream. For reference, the diameters employed during the flow tests were of 0.6mm and 2.4mm, for pipelines of 28mm and 150mm, respectively. The air-water data from the 28mm pipeline were compared against data taken with parallel-wire resistive sensor (Wong and Ooi, 1996). Either technique reproduced, within 3% precision interval, the same slug flow mean characteristics: bubble velocity, slug length, bubble length and frequency. This result is considered satisfactory and disclosed that this novel capacitive sensor detects the phase change almost locally, as do the parallel wire resistive sensor. This is a favorable feature of it, once most of the non-intrusive capacitive sensors have a sensitive length of two to ten pipe diameters (Elkow and Rezkallah, 1996).

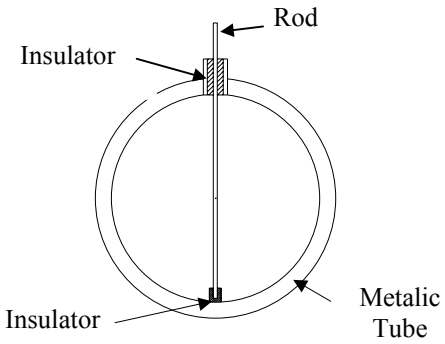

Figure 1 – Capacitive probe

3. Numerical determination of the electrostatic potential, V

The working principle of the capacitive sensor is electrostatic. The electrostatic potential field satisfies the Maxwell equation:

$$\varepsilon_0 \vec{\nabla} . k \vec{\nabla}(V) = \psi , \tag{1}$$

where ε_0 is the air dielectric constant, k is the oil permittivity, V is the electrostatic potential and ψ is the electrostatic charge flux. For educational purposes it is useful to draw attention to the similarity between the electrostatic and the heat conduction phenomena. Both are represented by the Poisson equation, and, if ε_0 is unity for the thermal problem, then k is the thermal conductivity, V is the temperature field and ψ represents the volumetric heat sources or heat sinks. Once the oil and the gas surrounding the electrodes (the rod and pipe wall) are a dielectric media, there is no net charge between them. Therefore, $\psi = 0$ and Equation (1) reduces to the Laplace equation.

The electrostatic potential field, V, is determined numerically using the finite volume technique embodied on the Phoenics 3.5.1 CFD code (Spalding, 1994). The domain is the electrical conductive rod and the electrical conductive tube, partially filled by two dielectrics: air and oil, as shown in Figure 2. The tube is 29mm in diameter, and 233mm long (which is equivalent to 8 tube diameters). The lengthwise domain distance is considered enough to not disturb the rod's potential field. Actually, the numerical simulations indicate that the field spans within one tube diameter from the rod. The rod is placed at mid distance from the domain ends, along the pipe diameter line. It is 0.6mm in diameter and 29mm long. The boundary conditions are: the tube walls are held at V=0 (grounded tube), the pipe ends are insulated (the potential's normal derivative is null), and the rod is kept at a constant potential of V = 12 (oscillator output voltage, see Fig. 5). Inside the pipe, the control volume's properties have either the electric permittivity of the air or of the oil, simulating variations of the oil level. The whole problem is setup within structured Cartesian grid, with special treatment at the curved solid boundaries of objects such as the rod or the oil level. The grid has a non-uniform spacing becoming finer near the rod where the potential gradients are greater. The grid size along the X, Y and Z directions is, respectively, 66x42x94 control volumes.

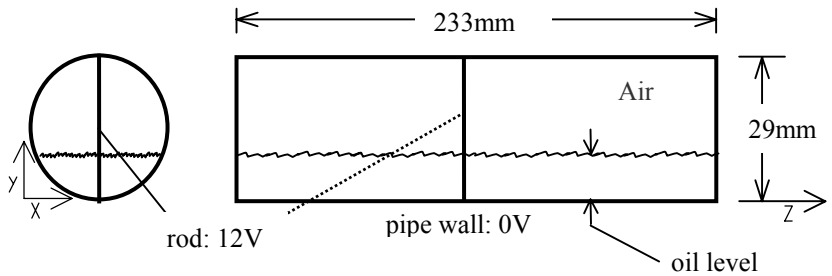

Figure 2 Domain size

Numerical results for the electrostatic potential field were determined by changing the oil level from zero up to one pipe diameter, along 8 equally spaced levels. Figure 3 shows the electrostatic field on the YZ plane, for X=14,5mm, when the oil fills 44% of the pipe diameter. The in-sets on the right side of Figure 3 represent electrostatic field cuts on the XZ plane, for Y=4mm, Y=14mm and Y=24mm, bottom to up. As one notices, presence of the oil and air do not disturb the electrostatic field. Actually, the dielectric constants of the air and the oil are 1.00054 and 2.437, respectively, pretty close from each other to introduce anisotropic effect on the media. The potential field near the rod is represented by concentric cylindrical surfaces and, at greater distances from the rod ovary shapes better represent it. The XZ cuts disclose axis-symmetric electrostatic fields, changing only along the radial direction. These are reasonable properties of the electrical field, given the pipe to rod diameter ratio of 48:1.

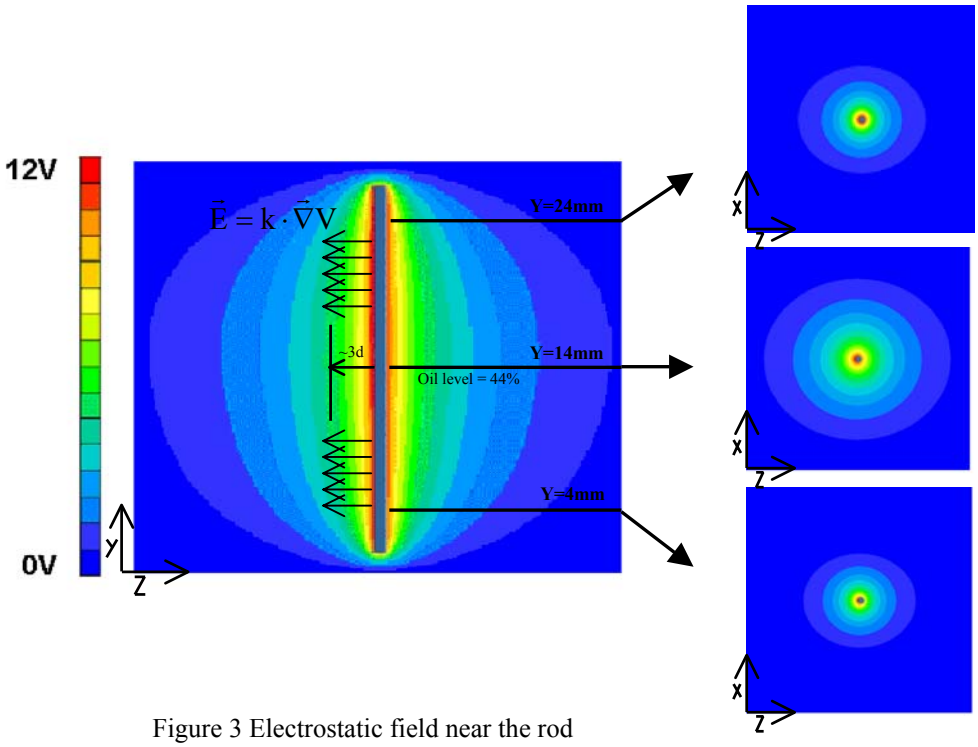

Figure 3 Electrostatic field near the rod

The decaying rate of the potential field is intense near the rod. There is a 50% voltage drop within the distance of three rod diameters, as shown on the left side of Fig. 3. As the potential field decays near the rod, the smaller is the probe sensitivity to dielectric changes far away from it. In other words, the probe samples a volume, which is confined within a small radial distance from the rod, what leads to an almost localized measurement along the diameter line of the rod.

Another interesting aspect revealed by Fig. 3 is the almost cylindrical and concentric iso-potential surfaces near the rod (except near its ends). In this region, the electric field vector is almost uniform and normal to the rod's surface. Therefore, it is expected that the charge density within the rod is nearly constant, once uniform electric field comes from uniform charge distribution. This reasoning is true when only one dielectric is present. When two dielectrics are present, witch is the case, and a uniform and normal electrical field still exists, is necessary that the rod's side wetted by the oil has a charge density greater than the side embedded by the gas. This is because the oil dielectric constant is greater than the one from the air. The capacitance is proportional to the net charge, which, by its turn, is proportional to the charge density, to the dielectric constants, and to the wetted and embedded extent of the rod. Therefore, it is expected that the capacitance varies linearly with the oil level.

4. Capacitance estimate

Even though the capacitance numerical prediction is accurate and reliable, very often it is not at hand for the electronic circuit designer. It requires skilled personnel on numerical methods. For design purposes, quick estimates of the probe output capacitance are convenient. In this section, a simplified model is proposed to draw quick capacitance estimates. The model consists in approximate the capacitance between the rod and the pipe wall to the one produced by a line of charge. The line of charge has an infinitesimal diameter, and its length is ℓ, and is coincident with the pipe diameter D. The line has the charge uniformly distributed along its length. A charge density ρ is defined as the ratio between the rod's charge and its length, Equation (2):

$$\rho = q/\ell \,. \tag{2}$$

The model assumes axis-symmetric electrostatic field, such that the iso-potential lines are properly described using a cylindrical-polar coordinate system, (r,z). The rod's surface is approximated by the shape of an iso-potential line passing through the point S1 (d/2,0), where d is the rod diameter. The pipe's surface is approximated by the shape of an iso-potential line passing by point S2 (D/2,0), where D is the diameter of the pipe. See Figure 4. The capacitance estimate is done taking the ratio between the charge q and the electrostatic potential difference between the rod and the pipe wall.

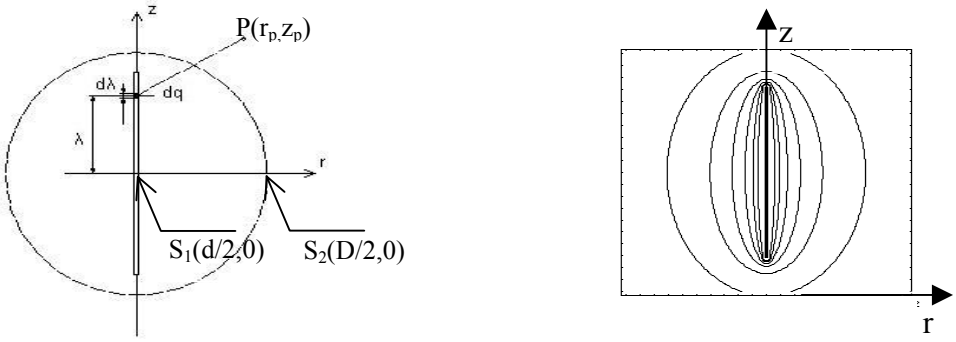

Figure 4 Line of charge model

The increment on the electrostatic potential at the point $P(r_p,z_p)$, resultant from the infinitesimal charge dq at position λ on the rod (see the left side of Figure 4), is:

$$dV = dq/4\pi\varepsilon_0 p \quad \text{where} \quad p = \sqrt{(z_p - \lambda)^2 + r_p{}^2} \tag{3}$$

The electrostatic potential at a point $P(r_p,z_p)$ results from the contributions of all infinitesimal charges distributed along the rod, and it is determined by the integral:

$$V(r_p, z_p) = \frac{\rho}{4\pi\varepsilon_0} \int_{\ell/2}^{\ell/2} \frac{d\lambda}{\sqrt{(z_p - \lambda)^2 + r_p{}^2}} \equiv \frac{\rho}{4\pi\varepsilon_0} \text{Abs}[\text{ArcSinh}(\frac{z_p + \ell/2}{r_p}) - \text{ArcSinh}(\frac{z_p - \ell/2}{r_p})] \tag{4}$$

At the right side of Figure 4, the iso-potential lines are shown. In fact, they are axis-symmetric, and their ovary shapes are similar to the ones found by numerical simulation (Fig. 3). The capacitance C is defined in Eq. (5), as the ratio between the rod's charge and the voltage difference between S_1 and S_2. Employing Eq.(4) to determine this voltage difference, taking $\ell = D$, and observing that $\ell/d \cong 50 >> 1$, the final result is approximated by:

$$C = \frac{q}{\Delta V} = \frac{\rho.\ell}{\frac{\rho}{4\pi\varepsilon_0}.[2.\text{ArcSinh}(\frac{\ell}{2.r})|_{D/2}^{d/2}]} = \frac{2\pi\varepsilon_0\ell}{\text{ArcSinh}(\frac{\ell}{d}) - \text{ArcSinh}(1)} \approx \frac{2\pi\varepsilon_0\ell}{\ln\left[\frac{2}{1+\sqrt{2}}\left(\frac{\ell}{d}\right)\right]} \tag{5}$$

Equation (5) is an analytical expression to estimate the sensor's capacitance. Accordingly to Eq. (5), the capacitance grows almost linearly with the rod's length ℓ, and decreases logarithmically as the rod's diameter increase. The validity of this approximation is shown on section 6, where the experimentally determined capacitance as well as the numerical and the estimated value are compared.

5. Circuit model and block diagram

The capacitive sensor circuit is schematically represented in the left side of Figure 5. An AC voltage of 12 V and 150 KHz, delivered by the oscillator, feeds the circuit, constituted by the low impedance charge resistor Rc, the capacitive sensor C (rod and pipe walls), the background circuit capacitance Cp, and the resistor Rp, representing a possible current leakage through the liquid. The output voltage, Vc, feeds a signal conditioner, which will be further discussed. Vc is proportional to the current ic, which is determined by Eq. (6):

$$i_c = (C + C_p)(dV/dt) + V/R_p \quad \text{where } V=A.\text{sen}(\omega t) \tag{6}$$

The background capacitance is an undesirable capacitance created within the circuit tracks and along the connection wires from the circuit to the probe. Its net effect is to introduce a DC level on the capacitance measurement. Current leakage between the probe and the liquid may occur if the liquid is electrically conductive. The emulsions of salty water in oil are an example. The resistor Rp represents the net effect of the current leakage on the circuit. For oil and gas, Rp has a very high value, and does not drain current.

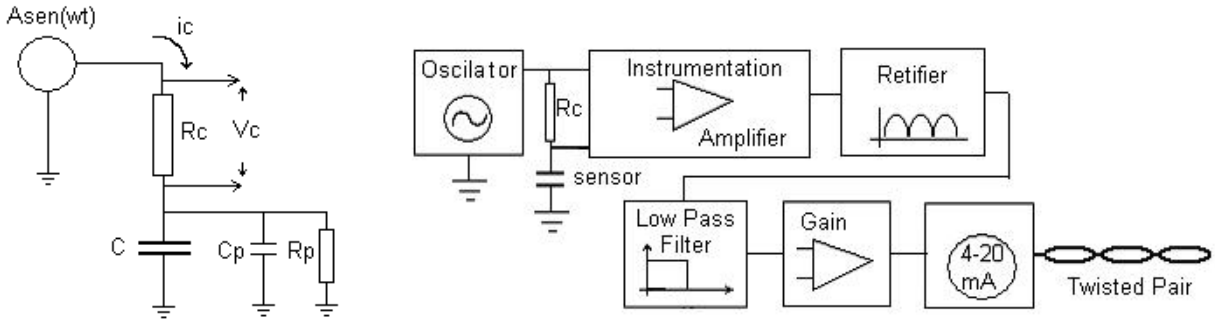

Figure 5 Circuit model and block diagram

The capacitance variation due to the intermittent passage of gas and liquid by the rod causes a signal amplitude modulation on the output voltage, Vc. The modulated signal is delivered to the signal conditioner, as shown in the right side of Figure 5. Then it is rectified and filtered by a low-pass filter with cut-off frequency of 1KHz, three orders greater than the characteristic slug frequency. The low pass filter delivers the signal to an amplifier, which, by its turn, feeds a voltage to the current converter. The output is a 4-20mA current, transported to the acquisition system through twisted pair of wires.

6. Static tests

The purpose of the static tests is the determination of the system sensitivity, the background capacitance, the response to the oil level inside the pipe and, at last, the effects of temperature on the signal output. The liquid used was petroleum from Campos's basin, identified as Marlin 10. The oil density is 917 kg/m^3 and the measured permittivity is 2.437 at 25^{o}C. The oil permittivity remained constant when the temperature increased up to 50^{o}C. The signal conditioner sensitivity was measured replacing the probe by a commercial capacitor with nominal value of 1pF, and then measuring its output voltage, prior to the amplification modulus. The measured sensitivity is of 0.14V to 1pF. The background capacitance was estimated as 1.86 V, or 13.2 pF.

The tests of the system response to the oil level started by measuring the sensor output when the 150mm pipe was either full of air or full of oil. The experimentally determined capacitances are in Table 1, along with the numerically and analytically estimated capacitances. Considering the tube full of air, the capacitance deviation of the experimental from the numerical and analytical are of -7% and -22%, respectively. On the other hand, considering the tube full of oil, the deviations fall to +2% and -15%. The analytical expression renders estimates 20% imprecise. Nonetheless, it is useful for circuit design. The second line shows a comparison between numerically obtained and analytically estimated capacitances. No experimental capacitance measurements were done with the 29mm diameter pipe.

Table 1 – Experimental, numerical and estimated capacitance for tubes of 150mm and 29mm, filled with air and oil.

Pipe Diameter (mm)	Fluid	Experimental Capacitance (pF)	Numerical Capacitance (pF)	Anal. Estimated Capacitance (pF)
150	Air	2.7	2.5	2.1
	Oil	6.0	6.1	5.1
29	Air		0.5	0.4
	Oil		1.2	1.0

The sensor's output voltage against the changes of the oil height inside the 29mm diameter tube was determined using the experimental apparatus in Fig. 6. It consists of a 29mm diameter steel pipe 1000mm long and held horizontal. The pipe is initially full of oil at ambient temperature. The oil level is changed by draining the oil from the tube. After

draining certain volume the valve is closed and the static oil level is measured by the micrometer placed at the top of the tube. The readings of the output voltage and the oil level are in Fig. 6(b). They exhibit a linear behavior as predicted in sections 4 and 5.

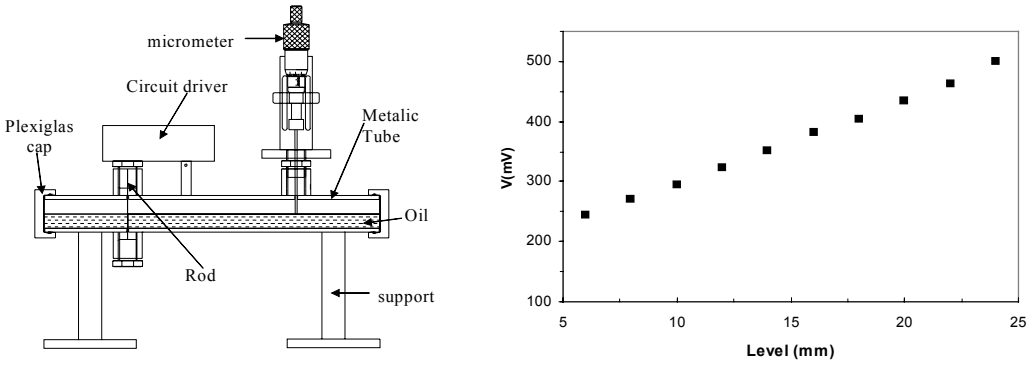

Figure 6 Static setup to determine the capacitive sensor output as function of the oil level

At last, it is presented the effect of temperature variation upon the output signal. The temperature sensitivity is concerned to the circuit only, since the oil and the air permittivity are practically constant within 20°C to 45°C. The circuit was inserted into a chamber with controlled temperature. The probe capacitance was again replaced by a 1pF commercial capacitor. As the chamber temperature spanned from 30°C to 45°C, the circuit's output was recorded. While the capacitance was kept constant (1pF), the voltage output increased 350 mV. Consequently, the circuit sensitivity to temperature is approximately 0.13pF/°C.

The main drawbacks of the circuit are the background capacitance and its temperature sensitivity. The first introduces a DC level on the amplification stage, which frequently causes the signal saturation. The second is nearly 10% of the capacitance of the 29mm diameter pipe, representing a large percentage for small pipe setups. The first drawback can be eliminated introducing an offset voltage to cancel the background capacitance. The second is hard to cope if one intends to use the developed capacitive sensor as a level transducer or as liquid holdup transducer. At the present moment the instrument is used as a phase detector and the temperature sensitivity has no main role, since its effect is canceled during signal processing by normalizing the output voltage.

7. Dynamic tests

Two dynamic tests were taken. One indoor, employing the experimental facility of the Energy Department, and the other using the Eng. Baruzzi test facility of Petrobras, located in Atalaia, SE.

The indoor facility consists of a 29mm horizontal steel pipeline 26280mm long, with maximum operational pressure of 9 Barg. Marlin 10 oil and nitrogen were injected upstream horizontal test section. The selected oil and gas flow rates arouse slug flow pattern along the first 100 line diameters. The test section is placed at 777 line diameters, downstream the gas injector. Two capacitive sensors were installed, 2 pipeline diameters distant from each other, producing a twin signal.

The second facility uses a horizontal 150mm diameter pipe 200m long. During the tests, natural gas and a blend of Camorin and Sergipe Terra oils were employed. The line maximum operational pressure was of 15 Barg. The selected oil and gas flow rates arouse slug flow pattern along the line. Two capacitive sensors were installed at 1100 pipeline diameters downstream the gas injector, spaced from each other 2 pipe diameters.

During both tests, the signal outputs were acquired by an IBM-PC equipped with a National Instrument acquisition system, encompassing a 32 channel multiplexer, a SCXI 1100 amplifier, and an AT-MIO-16E10 board.

Figure 7 displays the twin signals as a function of time. Fig. 7(a) corresponds to the 29mm diameter pipeline and Fig. 7(b) to the 150mm diameter pipeline. The high and low voltage signals correspond to the passage of the liquid piston and the gas bubble, respectively. The twin signals (blue and pink lines) are delayed due the axial displacement between the two capacitive sensors. They clearly identify the gas and liquid structures, and show how the events evolve in time. Fig. 7(a), for example, shows the start of a bubble coalescence. The voltage spans are of 1V and 4V for Fig. 7(a) and Fig. 7(b), respectively. The increase on the voltage span for the signal of Fig. 7(b) is due the bigger size of the rod's length. Despite of this characteristic, there is no other distinguishable feature between the signals when the pipe diameter changed from 29mm to 150mm.

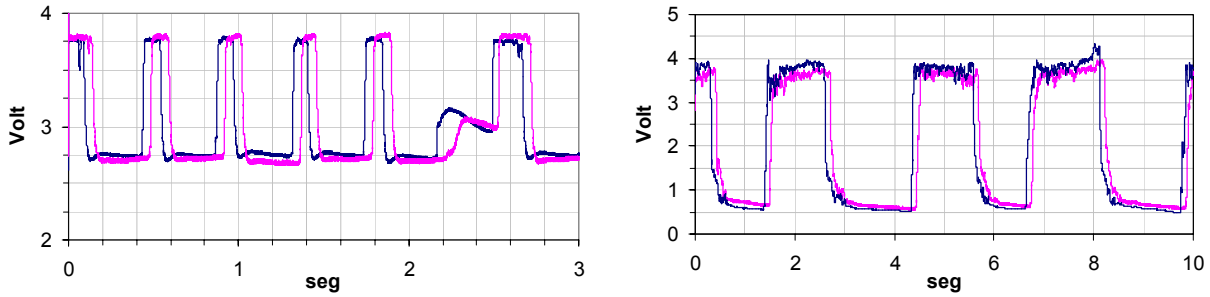

Figure 7 - Voltage signal as a function of time for slug flow
(a) Left, 29mm diameter tube, superficial liquid and gas velocities 17cm/s and 67cm/s
(b) Right, 150mm diameter tube, superficial liquid and gas velocities 67cm/s and 70cm/s

The time delay in Fig. 7 is easily measured, and from it is possible to determine the front bubble velocity, the liquid slug and bubble lengths, as well as the bubble frequency. These relevant properties of the slug flow are show in Figure 8, in form of histograms. They illustrate the capabilities of the developed capacitive sensor. The data come from 29mm diameter pipeline, operating with Marlim 10 oil and nitrogen, at superficial liquid and gas velocities of 17 cm/s and 67 cm/s, respectively.

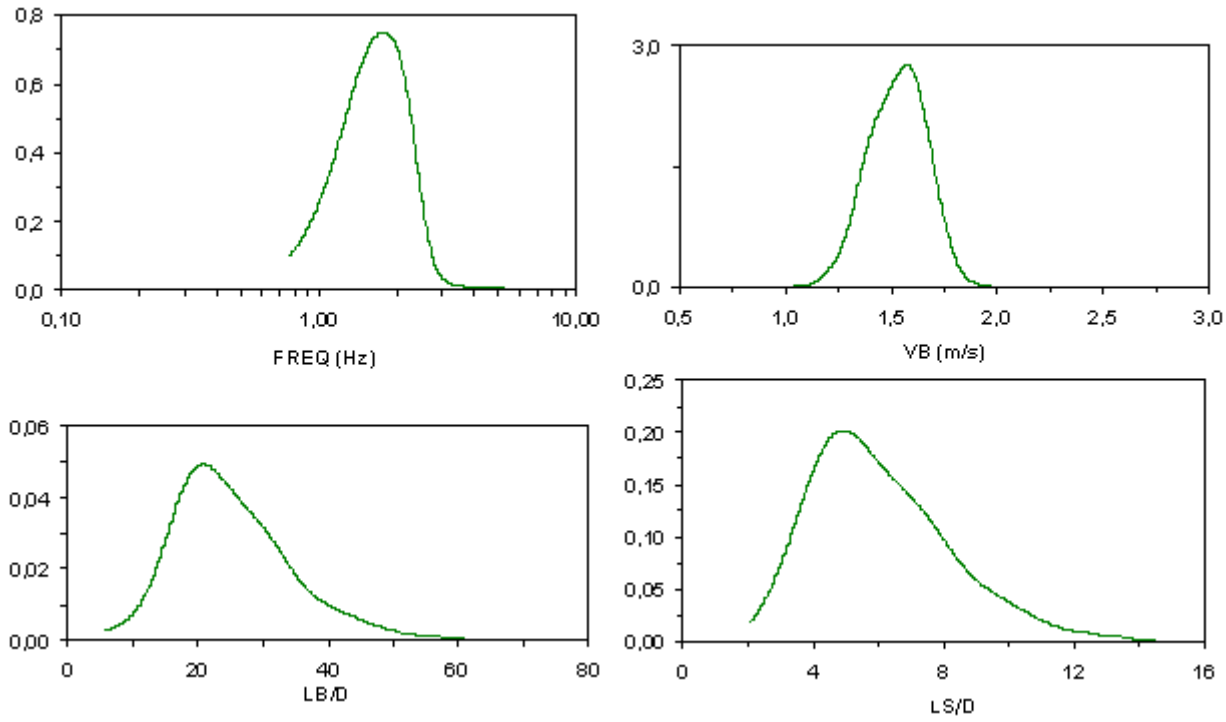

Figure 8 Bubble frequency, bubble velocity, bubble length and slug length histograms

8. Conclusions

This paper presents a novel configuration for intrusive capacitive sensors, where the pipe wall is an active part of the system, that is, one of the electrodes, and the other is a metallic rod inserted inside the pipe. This configuration proved to work well in gas-oil pipelines, fulfilling the safety regulations and requiring small changes to adapt the pipeline to the instruments.

The developed probe is a slender rod with length to diameter ratio typically 50:1. The electrostatic potential field near the rod is axis-symmetric, as shown by the numerical simulations. The electrostatic potential decays 50% within a distance equivalent to 3 rod's diameter, indicating that the sensor sensitivity is to local events. An estimate of the capacitance was developed from a simpler geometric configuration. The analytical expression quickly draws capacitance estimates within 20% error, which are useful for circuit design purposes. It also disclosed that the capacitance increases linearly with the rod's length and logarithmically with its diameter. The sensitivity of the circuit is of 0.14V per pF without signal amplification. The capacitance variation when the pipe is full of air or full of oil is, typically, 1pF or 4pF, accordingly, when the pipe diameters are of 29mm or 150mm. The static tests showed a linear

relationship between the output voltage and the oil level inside the pipe. It also disclosed a temperature sensitivity of 0.13pF per degree Celsius and a background capacitance of 13.2pF. These two last features are the major drawbacks and are certainly to be improved on future designs. Despite of these negative aspects, they do not interfere with the gas-liquid phase detection. The dynamic tests with 29mm and 150mm diameter pipes were successfully conducted, and the output signals of the capacitive sensor rendered important slug flow parameters such as: bubble velocity and length, bubble frequency and slug length

9. Acknowledgements

The authors N. Mastelari, M. Zwanziger and E.S. Rosa would like to thank to Petrobras to support this research under the contract number 0050.0001159.04.2 and also thanks to MSc. Marcelo Gonçalves and Dr. José Roberto Fagundes Netto from Petrobras for the useful suggestions and encouragement.

9. References

Abouelwafa-Razzak, A., Kendall, E.J.M., 1980, "The use of Capacitance Sensors for Phase Percentage Determination in Multiphase Pipelines", IEEE Transactions of Instrumentation and Measurement, vol. 29, n.1, pp. 24-27.

Duarte L.G.C., Prata A. T., 2002, "Geometria de Sensores Capacitivos Aplicados em Escoamento Multifásicos", II Congresso Nacional de Engenharia Mecânica- CONEM, João Pessoa, 2002.

Elkow K.J. and Rezkallah, K.S., 1996, "Void Fraction Measurements in Gas-Liquid Flows Using Capacitance Sensors", Meas. Sci. Techol. Vol 7, 1153-63.

Heerens, W.C., 1986, "Application of Capacitance Techniques in Sensor Design", J. Phys. E: Sci. Instrum. 19, pp 897-906.

Merilo, M., Dechene, R.L. and Cicowlas, W.M., 1977, Void Fraction Measurement With a Rotating Electric Field Conductance Gauge", J. Heat Transfer Trans. ASME, 99 330-1

Masuda Y., Nishikawa M. and Ichijo B., 1980, "New Methods of Measuring Capacitance and Resistance of Very High Loss Materials at High Frequencies", IEEE Trans. Instrum. Meas, 29, 28-36

Reis, E., Goldstein, L. 2003, "A New Probe for Measuring the Gas-Liquid Interface Profile", 17th International Congress of Mechanical Engineering.

Spalding, D.B., 1994, "The PHOENICS Encyclopedia", CHAM Ltda., London, U.K

Wong, T.N., Ooi,K.T., 1996, "Performance of a Parallel-Wire Deph Probe", International Communication of Heat and Mass Transfer, v.23, n.7, p. 1003-1009.

10. Responsibility notice

The authors N. Mastelari, M. Zwanziger and E.S. Rosa are the only responsible for the printed material included in this paper.